River Flow 2020 – Uijttewaal et al (eds)
© 2020 Taylor & Francis Group, London, ISBN 978-0-367-62773-7

Effects of irregular particle shapes on the sediment movement and transport rate in gravel-bed channels

Takatoshi Atsumi
Graduate School of Science and Engineering, Chuo University, Tokyo, Japan

Shoji Fukuoka
Research and Development Initiative Chuo University, Tokyo, Japan

ABSTRACT: The numerical movable-bed experiments were conducted to investigate the effect of particle shapes on the transport of gravel particles. The river-bed materials used in the numerical experiment were three kinds of particles with the same nominal diameter (70 mm) and different shapes (Thin, Rod, Sphere). The analysis of the fundamental movement process of sediment transport revealed the importance of particle shape on the pick-up process in comparison with the particle velocity. Non-spherical particles form the imbrication and clusters which make the river-bed stabilize, and reduce the pick-up volume compared to that of spherical particles. In particular, the difference in the pick-up rate between thin and rod particles is considerable under high tractive force.

1 INTRODUCTION

The gravel-bed river is composed of particles of various shapes and sizes and takes the imbrication form which makes the river-bed stable. The shape and size of gravel particles are considered to be significant on river-bed structure and sediment transport rate. For example, Gomez (1994) pointed out that the increasing roughness of a stable armor changed due to the particle shape. However, quantitative effects of shapes on bed variation and sediment transport have not been clarified because it is difficult to measure the mechanism of particle motions during floods. In addition, because particle size and shape that could be used in hydraulic experiments are limited, the results of hydraulic experiments could not provide sufficient knowledge on the effect of particle shapes. Fukuoka et al. (2014) constructed a numerical movable-bed channel that takes account of dynamic interactions between flow and particles using gravel particles in different sizes and shape. They conducted numerical movable-bed experiments with sphere particles and gravel particles and clarified effects of particle sizes and shapes on sediment movement and sediment transport rates. Fukuda & Fukuoka (2017) applied their model to the debris flow experiment. The investigation by Fukuda & Fukuoka (2017) showed that this model could reproduce distribution of the particle velocities and discharge rates of water and particles in hyperconcentrated flows. The investigation of Fukuoka et al. (2014) was difficult to consider the influence of each particle shape on particle motion because numerical movable-bed experiments with five different shapes and sizes particles. Therefore, the present numerical movable-bed experiments are conducted using three kinds of gravels with uniform particle sizes of different shapes, which facilitate to understand the influence of particle shape.

2 NUMERICAL METHODS

The numerical simulation model of Fukuoka et al. (2014) is used. This model can simulate three-dimensional motions of flows and gravel particles in different shapes and sizes. Fluid

motions were simulated using the governing equations of a single-fluid model for the solid-liquid multiphase flows in the Eulerian approach. Particle motions were computed as rigid bodies with the Lagrangian approach using DEM method.

2.1 *Fluid motions*

The fluid motions are calculated using the governing equations used in a single-fluid model for solid-liquid multiphase flows in the Eulerian approach. The Smagorinsky model was used as the subgrid scale turbulence model.

$$\frac{\partial ui}{\partial xi} = 0 \tag{1}$$

$$\frac{\mathrm{D}u_i}{\mathrm{D}t} = g_i - \frac{1}{\rho}\frac{\partial P}{\partial \mathrm{x}_i} + \frac{\partial}{\partial \mathrm{x}_i}\left\{2(\upsilon + \upsilon_t)S_{ij}\right\} \tag{2}$$

$$S_{ij} = \frac{1}{2}\left(\frac{\partial u_i}{\partial x_j} + \frac{\partial u_j}{\partial x_i}\right) \tag{3}$$

$$\upsilon = \mu/\rho \tag{4}$$

$$\nu_t = (C_s\Delta)^2\sqrt{2S_{kl}S_{kl}} \tag{5}$$

where u_i = i-th component of the weighted average velocity within a fluid cell; p = sum of the pressure and isotropic component of SGS stress; ρ = volume-averaged density; μ = volume-averaged viscosity; g_i = gravitational acceleration; v_i = SGS turbulent viscosity; S_ij = strain rate tensor; $\mathrm{C_s}$ = Smagorinsky constant; Δ = computational grid size.

The free-surface variation was simulated using the continuity equation of the fluid volume fraction f based on the volume-of-fluid (VOF) method.

$$\frac{\partial f}{\partial t} + \frac{\partial f u_\mathrm{i}}{\partial \mathrm{x}_\mathrm{i}} = 0 \tag{6}$$

2.2 *Particle motions*

Gravel particles were modeled by connecting several small spheres without gaps. The particle motion was simulated using the following momentum and angular momentum equations as a rigid body:

$$M\ddot{r}_i = Mg_i + F_i^f + F_i^c \tag{7}$$

$$\dot{\omega}_{i'} = I_{i'j'}^{-1}\left\{R_{j'i}\left(T_i^f + T_i^c\right) - \varepsilon_{j'k'l'}\omega_{k'}I_{l'm'}\omega_{m'}\right\} \tag{8}$$

where index i = the components of the global coordinate system fixed on the space; the indices i'-m' = the components of the local coordinate system fixed on a rigid body; M = mass of a particle; g_i = gravitational acceleration; r_i = position of the center of gravity of the rigid; F_i = force acting on the surface of the particle; suffix f, c = components of the fluid forces and contact forces between particles, respectively; ω_i = angular velocity; T_i = torque on the center of the gravity generated by the force; $I_{i'j'}^{-1}$ = inverse of the matrix consisting of the components of the moment of inertia tensor in the local coordinate system; $R_{j'i}$ = equal to $\mathrm{e}_{j'}\mathrm{e}_i$ ($\mathrm{e}_{j'}$ and $\mathrm{e}_i$are unit basis vectors); $\varepsilon_{i'j'k'}$ = Levi-Civita symbol. The basis vectors were simulated by using the angular velocity for the next time step solved by Eq.(9) and the time step Δt^p. The positions of the small spheres in the next time step with respect to the global

coordinate system were computed using the initial components of the positions of the small spheres in the local coordinate system, the basis vectors that were computed at every time step, and the center of gravity of the rigid body that was estimated on based on Eq.(8). Quaternion was used for the rotation of the basis vector, and the local coordinate systems using $R_{j'i}$ (Ushijima et al., 2008).

The parameters used in the simulations are shown in Table 1.

Table 1. Simulations parameters.

$\Delta x,\Delta y,\Delta z$: the size of the fluid computation cell	0.01	m
Δt^f: Time step for the fluid simulation	5.0×10^{-4}	s
Δt^p: Time step for the particle simulation (Case1/Case2,Case4/Case3)	$2.5 \times 10^{-6}/3.3 \times 10^{-6}/2.5 \times 10^{-6}$	s
ρ_w: Density of water	1000	kg/m^3
ρ_p: Density of particles	2650	kg/m^3
μ_w: Fluid viscosity	8.9×10^{-4}	Pa·s
Cs: Smagorinsky constant	0.173	-
E: Elastic modulus	5.0×10^{10}	Pa
pos: Poisson's ratio	0.33	-

3 NUMERICAL MOVABLE-BED EXPERIMENT

3.1 *Experimental conditions*

Particle shapes used in numerical experiments imitate particles in a real gravel-bed river. On the sand bar of the Asa river 2.3 km, 50 gravels were collected by the line grid method, and measured the longest axis a, the intermediate axis b and the shortest axis c are shown in Figure 1. The solid line indicates the Shape Factor $(c/(ab)^{0.5})$. The gravels are in the range of 0.4 ~ 0.6. Figure 2 shows Thin particle and Rod particle modeled by small spheres, which represent particles having a shape factor in the range of 0.5 ~ 0.6. Thin particle in Figure 2a have a rugged surface, and rod particle in Figure 2b have a smooth surface. The two types of particles have the same volume, and the nominal diameter estimated as a sphere of the equal volume is 70 mm. The two model particles and the gravels collected in the Asa river are plotted in Figure 1.

The numerical movable-bed channel and the coordinate system are shown in Figure 3. The numerical channel is 15 m long, 1 m wide with a bed slope of 1:20. The particles were packed randomly to make a river-bed. Table 2 shows the experimental conditions. Four numerical movable-bed experiments were conducted, and the thin particle was used in Case1, the rod particle in Case2, mixture of these two particles in Case3 and sphere particle in Case4. The

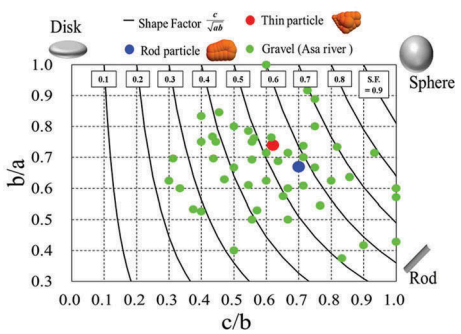

Figure 1. Characteristics of particle shapes.

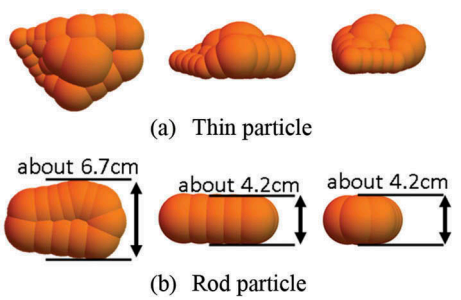

Figure 2. Particle shape viewed from different directions.

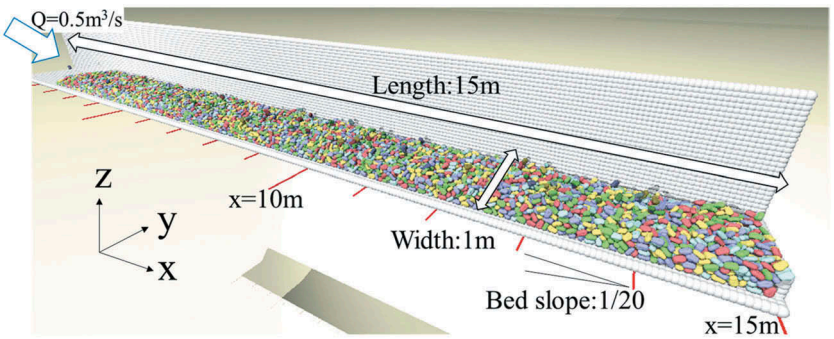

Figure 3. Numerical movable-bed channel and the coordinate system.

Table 2. Experimental conditions (Case1 ~ Case4).

	Case1	Case2	Case3	Case4
Water discharge [m3/s]	0.5	0.5	0.5	0.5
Water depth [m]	0.24	0.23	0.24	0.25
Froudeanumber(t=100s)[-]	1.27	1.35	1.31	1.25
Particle shape	Thin	Rod	2Shapes (Thin,Rod)	Sphere
Norminal diameter [mm]	70	70	70	70
Packing depth [m]	0.23	0.21	0.22	0.22

volume of packed particles was equal in all cases. In Case3, the same amount of thin and rod particles was mixed. The water discharge of 0.5 m^3/s was supplied to the channel, and the pressure was set to zero at the downstream end. The same number and volume of particles discharging out from the end of the channel were dropped back simultaneously to a section (x = 1~3m) near the upstream end of the channel. The water depth and the Froude number in Table 2 are spatially averaged values at x = 5 ~ 11 m.

3.2 *Transported volume of gravel particles*

Figure 4 Shows the volume of gravel particles passed through the cross section at x = 11 m. The measurement was performed at t = 0 ~ 100 s while the river-bed remained almost plane. In Case4, the transported volume of spherical particles is extremely large compared to other particle cases. Unlike the non-spherical particle, the spherical particle has only one contact point. Therefore, the sphere is generally considered to be the most mobile shape. Comparing the volume in Case1(Thin) and Case2(Rod), Case2 is about 1.85 times that of Case1. The effect of the particle shape on the transport rate is large. The total transported volume in Case3(2 shapes) was approximate half of that in Case1 and Case2, and there is not much difference between thin and rod particles. This suggests that the transport volume of mixed gravels is affected not only the shape of the particle itself but also that of the surrounding particles. It was confirmed that the difference in particle shapes has a large effect on sediment transport rates. In order to clarify the cause of the difference, the fundamental movement process of the particle is analyzed below.

3.3 *Influence of particle shape on moving process of gravels*

In order to analyze particles in saltation movement on the gravel bed, the streamwise particle velocity in the x direction of 0.05 m/s or more were defined as moving particles. In addition, particles that have a speed of 0.05 m/s less due to collision between particles and continue to move further were counted as the moving particle. At t = 0 ~ 100 s and x = 10 ~ 11 m, these

moving particles were sampled at 0.1s intervals, and the moving velocity and the projected area in the x direction were analyzed. Figure 5 shows the particle moving speed in x direction divided by the friction velocity of the flow in Case1 ~ Case4. In each case, the mean velocity and the variation pattern of the moving particles show almost the same value. Figure 6 shows the frequency distribution of the projected area in the x direction of moving particles in Case1 (Thin) and Case2(Rod). The projected area in the x direction does not take into account the influence of shelter of other moving particles. From Figure 6, Case1(Thin) and Case2(Rod) take the peak near the mean value, which are roughly symmetrical distributions. In Case1 (Thin) and Case2(Rod), the mean value is approximately equal to the projected area of a sphere with a diameter of d = 0.07 m. Since the saltation movement are in irregular rotational motion, the projected area in the x direction on the average seems to be regulated by the particle volume. Figure 7 shows the unevenness distribution of the river-bed in Case1 ~ Case4. The unevenness distribution is close to the normal distribution, and the difference due to the particle shape is small. In addition, the existence probability of the unevenness is in the range around the mean value to the nominal diameter (0.07m). It is considered that to find the effect of the shape of the moving particle itself on the particle moving speed was difficult because the scale of the unevenness was almost the same as that of the moving particle. Figure 8 shows the frequency distribution of the dimensionless step length in Case1 ~ Case4. The number of samples in Case1 ~ Case4 was 322, 560, 367 and 707, respectively. In each case, it could be confirmed that the distribution almost follows the exponential distribution, which is the same as the previous study (e.g. Hill et al. 2010). Also, the mean step length of Case1 ~ Case4 is 2.07, 2.20, 1.95 and 1.76 m, respectively, which are almost the same.

3.4 *Influence of particle shape on pick-up of particles from the river-bed*

Figure 9 shows the pick-up volume at $t = 0 \sim 100$ s, $x = 10 \sim 11$ m in Case1 ~ Case4. The ratio of the pick-up volume in each case is almost the same distributions as the transported volume of gravel particles shown in Figure 4, the particle shape is a prominent effect in the pick-up process and river-bed structure. One of the hydro-geological phenomena characterizing non-spherical particles is the imbrication of the gravel-bed surface. Figure 10 shows the arrangement of particles on the river-bed surface before and after experiment. The imbrication is often seen at the bed surface in gravel rivers after floods where gravel's longest axis is directed toward the streamwise direction and slightly vertically upward. The imbrication takes a stable posture by directing the contact force to the upstream direction (Figure 11). In Case1 ~ Case3, the imbrication was clearly formed on the gravel bed. In addition, in Case1 ~ Case3, a group of clusters composed of several gravel particles are formed. Figure 12 shows the clusters formed in Case1. A group of gravel enclosed by circles is clusters. The cluster has a stable structure in a group against stream forces. Unless particles moving from the upstream collide with clusters, the cluster kept stable.

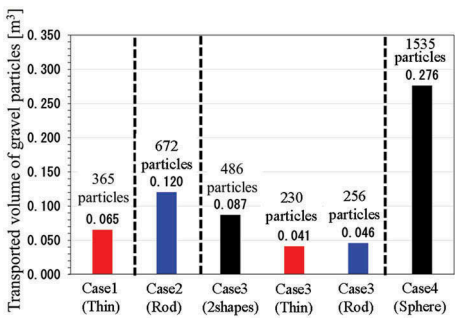

Figure 4. Volume of gravel particles passing through the cross section at $x = 11$ m.

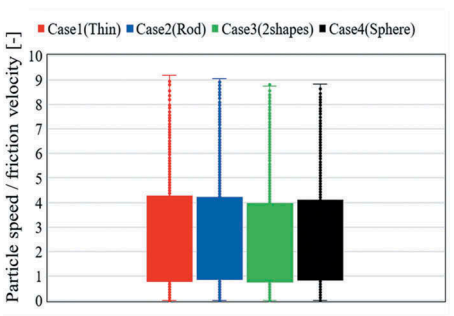

Figure 5. Particle moving speed.

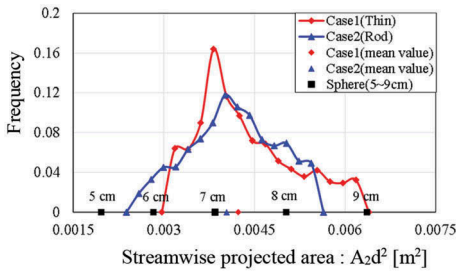

Figure 6. Frequency distribution of the projected area in x direction.

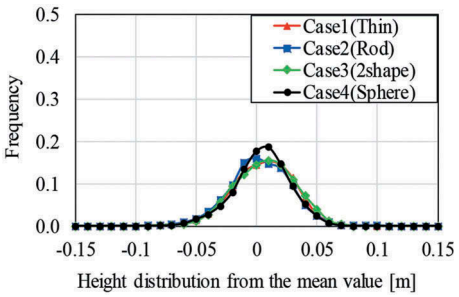

Figure 7. Frequency distribution of unevenness of the river-bed.

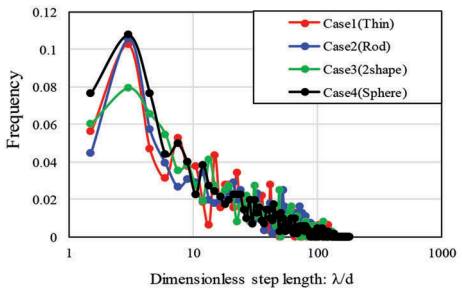

Figure 8. Frequency distribution of dimensionless step length.

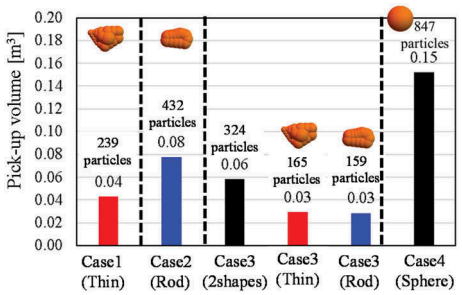

Figure 9. Pick-up volume at x = 10 ~ 11 m in the moveable-bed experiments.

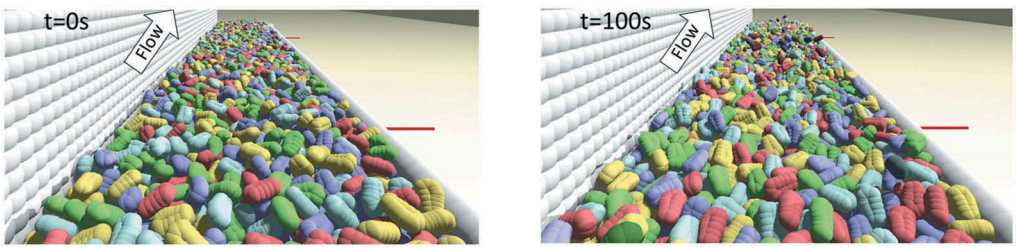

(a) t = 0 s (b) t = 100 s

Figure 10. Formation of the imbrication in Case2(Rod).

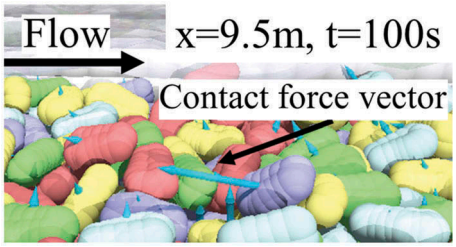

Figure 11. Posture of particles forming the imbrication.

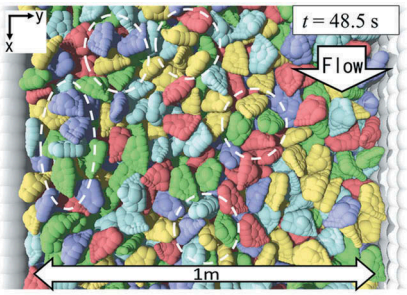

Figure 12. Formation of clusters in Case1 (Thin).

Additional numerical experiments were conducted to investigate the pick-up rate of thin, rod and spherical particles. The channel of the numerical experiment was 10 m, the width was 1 m, the bed slope was 1:20, and gravel particles are laid at a thickness of about 20 cm in the range of $x = 6 \sim 8$ m. In other sections of the channel, moving particles are laid only the surface layer. The discharge was increased from 0.1 ~ 0.5 m^3/s every 0.1 m^3/s and the pick-up rate was measured. Table 3 shows the friction velocity versus the discharge. The pick-up rate was calculated by examining the residual rate of tracer particles in the same way as Nakagawa & Tsujimoto (1976). Of the particles exposed on the moving bed surface $x = 6 \sim 8$ m and $y = -0.4 \sim 0.4$ m, particles that are higher level on the bed were selected as tracer particles. Similarly, for Case1 ~ Case4, tracer particles were selected at $x = 9 \sim 11$ m and $y = -0.4 \sim 0.4$ m at $t = 20$ s. Figure 13 shows that the bright color particles are tracer particles in CaseA(Thin). The number of tracer particles in each experiment is from 67 ~ 105.

Figure 14 shows the measured results of the pick-up rate. The friction velocity was calculated from $(gRI)^{0.5}$. The solid lines are CaseA(Thin), CaseB(Rod), and CaseC(Sphere), and the plots show the values measured in Case1 ~ Case4 of the movable-bed experiments. In case C (sphere), the pick-up rate increases at about $u_* = 0.230$ m/s, whereas the pick-up rate for non-spherical particles (CaseA and CaseB) increases around $u_* = 0.260$ m/s. Therefore, it

Table 3. Friction velocity [m/s] (CaseA ~ CaseC).

Water discharge [m^3/s]	0.1	0.2	0.3	0.4	0.5
CaseA(Thin)	0.194	0.220	0.254	0.266	0.283
CaseB(Rod)	0.202	0.228	0.252	0.273	0.298
CaseC(Sphere)	0.196	0.230	0.248	0.255	-

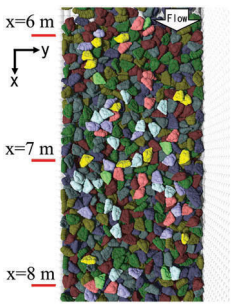

Figure 13. Bright color tracer particles in CaseA (Thin,0.5 m^3/s).

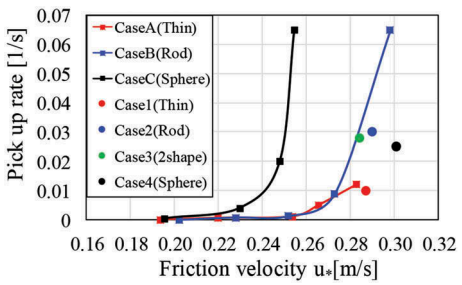

Figure 14. Pick-up rate versus friction velocity.

was confirmed that the critical friction velocity changes depending on the particle shape. Also, comparing CaseA(Thin) and CaseB(Rod), there is almost no difference at low tractive force near the critical tractive force. It is probable for both cases that there are a certain number of particles in unstable positions and they can easily dislodge from river-bed by the flow. On the other hand, in the high tractive force state, pick-up rates of CaseA(Thin) and CaseB(Rod) are clearly different. The thin particle has a large flat area and irregular shape, so the thin particle is easy to form clusters and is easier to transmit force to surrounding particles than rod particles. It was observed that particles just downstream of the cluster are picked up along with the collapse of the cluster.

The future study is to clarify the existence ratio of the cluster on the river-bed surface and cluster's roles to evaluate the pick-up volume.

4 CONCLUSIONS

Numerical movable-bed experiments with the same nominal diameter of three gravel particles were conducted in order to examine the effect of particle shapes on sediment transport. Main conclusions drawn are described as follows:

1. Significant differences in sediment transport mechanism and transported volume were caused by the difference in particle shape. Case4(sphere) has the largest volume of sediment transportation compared to the other cases, and the sphere is considered as the most mobile particle shape. The sediment transported volume in Case3(2 shapes) showed that the particle shape affects not only the motion of the particle itself, but also the motion of surrounding particles.
2. The moving speed of the saltating particles showed little difference depends on the particle shape and was almost the same mean value and variation pattern. Because the mean value of the projected area in each Case1(Thin) and Case2(Rod) do not differ much from the projected area of a sphere of the same volume. The mean step length was almost the same for four cases. The distribution of dimensionless step length (λ/d) was exponential.
3. It was found that the effect of particle shape clearly appears in the pick-up process from river-bed. Non-spherical particles in Case1 ~ Case3 formed the imbrication and clusters which make river-bed stable. The experiments to analyze the pick-up rate of thin, rod and spherical particles showed that the particles shape had a remarkable effect on not only the critical shear stress but also the pick-up rate under high tractive force of the flow. It is necessary to analyze the role of clusters on the river-bed in detail in order to evaluate the pick-up volume.

REFERENCES

Fukuoka, S., Fukuda, T. and Uchida, T. (2014). Effects of sizes and shapes of gravel particles on sediment transports and bed variations in a numerical movable-bed channel., *Advances in Water Resources*, Vol. 72, pp. 84–96.

Fukuda, T. and Fukuoka, S. (2017). Interface-resolved large eddy simulations of hyperconcentrated flows using spheres and gravel particles., *Advances in Water Resources*, Vol. 129, pp. 297–310.

Gomez, B. (1994). Effects of particle shape and mobility on stable armor development. *Water Resources Research*, Vol.30, No.7, pp. 2229–2239.

Hill, K. M., L. DellAngelo, and M. M. Meerschaert (2010), Heavy-tailed travel distance in gravel bed transport: An exploratory enquiry, *Journal of Geophysical Research*, Vol. 115, F00A14, doi: 10.1029/2009JF001276.

Nakagawa, H. and Tsujimoto, T. (1976). On probabilistic characteristics of motion of individual sediment particles on stream beds. *Proceedings of the 2nd International Symposium on Stochastic Hydraulics, International Association of Hydraulic Research*, pp. 293–316.

Ushijima, S., Fukutani, A. and Makino, O. (2008). Prediction method for movements with collisions of arbitrary-shaped objects in 3D free-surface flows, *JSCE Journal B*, Vol.64, No.2, pp. 128–138, in Japanese.